X International Conference on Computational Methods for Coupled Problems in Science and Engineering
COUPLED PROBLEMS 2023
M. Papadrakakis, B. Schrefler and E. Oñate (Eds)

ON THE 2D-1D COUPLING IN NUMERICAL SIMULATIONS OF SIMPLIFIED AIR FLOW MODEL IN HUMAN AIRWAYS

A. LANCMANOVÁ[⋆,†], T. BODNÁR[†,⋆], A. SEQUEIRA[‡]

[⋆] Institute of Mathematics , Czech Academy of Sciences
Žitná 25, Praha 1, 115 67, Czech Republic
e-mail: lancmanova@math.cas.cz, Web page: https://www.math.cas.cz

[†]Department of Technical Mathematics
Faculty of Mechanical Engineering, Czech Technical University in Prague
Karlovo náměstí 13, Praha 2, 121 35, Czech Republic
e-mail: Tomas.Bodnar@fs.cvut.cz - Web page: https://fs.cvut.cz

[‡]Department of Mathematics and CEMAT,
Instituto Superior Tecnico,
Av. Rovisco Pais, 1049–001 Lisbon, Portugal
e-mail: adelia.sequeira@tecnico.ulisboa.pt - Web page:
https://www.math.tecnico.ulisboa.pt/˜asequeir/

Key words: Navier-Stokes equations, reduced order model, coupling, air, respiratory system

Abstract. This paper presents selected results regarding the implementation, validation and testing of a simple 2D-1D coupled model designed to capture some essential features of the oscillatory air flow in human respiratory system. The model relies on a 2D flow model solved by a simple finite-difference scheme in the immersed boundary setting. The incompressible fluid flow from this model is coupled to a simplified 1D fluid-structure-interaction model simulating the flow in a tube with elastic walls. Some first results obtained using the coupled 2D-1D model in an oscillating (Womersley-like) type of flow are presented and discussed in detail. The influence of model parameters is explored for a range of physically relevant settings.

1 INTRODUCTION

This work is motivated by the air flow in the human respiratory system. From the mathematical modelling point of view this problem can be considered (with certain level of simplification) as flow of an incompressible viscous fluid in a system of branching channels. This leads to a complex multiscale problem, whose solution requires a large amount of complicated and time-consuming numerical calculations.

In order to better understand the problem and save some time with the implementation of the full-scale three-dimensional numerical simulations, a simplified (almost toy-like) model was developed, validated and tested. This model considers a 2D flow problem coupled to a reduced 1D FSI problem. The numerical methods and coupling algorithms were tested for a Womersley-like oscillatory flow (with periodically changing flow direction in time) coupled to a simple one-dimensional flexible tube model. The modeling and coupling issues are explored

hereafter. The main aim of this work is to test the model for the conditions and parameters close to those found in the human respiratory system. These settings are quite different from those in blood flows for which such model systems were typically developed. In addition, some effort is made to adjust the coupled model to a 2D flow problem in a rigid geometry, which is an unusual choice for this kind of models.

2 AIRFLOW IN THE HUMAN AIRWAYS

Numerous characteristic flow phenomena can be found in the human airways, such as merging streams, oscillating flows, turbulence, secondary flows, and separation [2]. Although it is a generally accepted assumption that most of the flows in respiratory system can be considered as laminar, few exceptions may occur [6].

The air flow in respiratory system is naturally unsteady, having a time-periodic oscillatory character. A human's normal *respiratory rate* for an adult at rest is between 10 and 15 *breaths per minute*, which corresponds to a Womersley number (Wo) between 2.41 and 2.95. Depending on the Womersley number, analytical velocity profiles, velocity gradient at the wall and volume flow rate can be computed based on an oscillating pressure gradient (pressure drop) [12]. An illustration of such time-periodic two-dimensional analytical solution is shown in Fig. 1. This

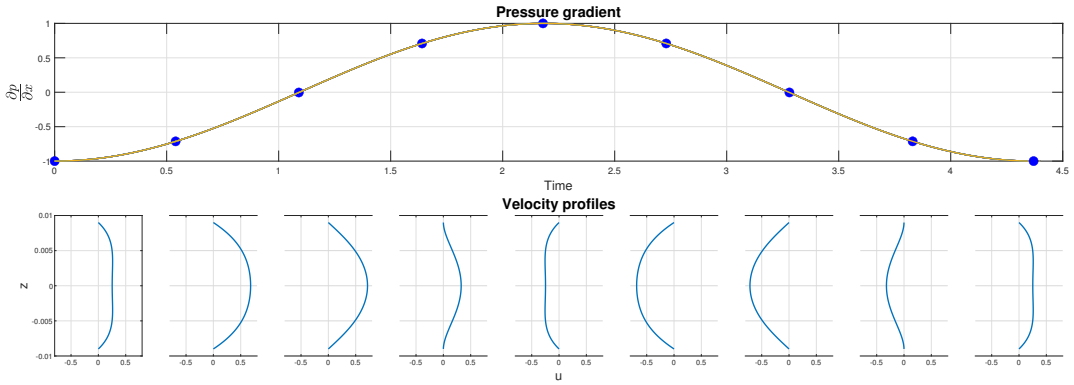

Figure 1: Velocity profiles for Womersley number 2.41.

analytical solution can be (and was) used for validation of the numerical code developed for unsteady flow simulations. It is interesting to observe the change of shape of the velocity profile over time, where certain profiles are quite far from the usual parabolic shape normally found in steady flows.

3 TWO-DIMENSIONAL FLOW MODEL

The work presented in this paper is based on the coupling of a 2D flow model with a simplified 1D Fluid-Structure-Interaction (FSI) model. The 2D model is the standard system of Navier-Stokes equations for an incompressible, Newtonian fluid. The system consists of linear momentum balance equations, complemented by the divergence-free incompressibility constraint, replacing the mass balance equations for constant density fluids.

This governing system of partial differential equations is solved by the finite-difference method in the immersed boundary approach. The modified (reduced numerical diffusion) Lax-Friedrichs scheme was used, together with the pressure correction method for velocity-pressure

coupling, employing a Jacobi solver for the discretized Poisson equation. More details about the implementation and validation of this numerical approach can be found in [4], [11].

4 ONE-DIMENSIONAL FSI MODEL

4.1 Governing equations

The simple one dimensional FSI model used in this paper describes the flow of an incompressible viscous fluid in an elastic tube. The tube is assumed to be axially (rotationally/radially) symmetric, having a cross-section that can vary in time and space, based on the difference between internal and external pressure. The 1D model is derived from the fully 3D incompressible Navier-Stokes equations coupled with a structure model for the vessel wall, by making some simplifying assumptions and integrating the variables over the cross section [9]. The resulting system of coupled evolutionary partial differential equations (1)-(2) for flow-rate $Q(x,t)$ and cross-sectional area $A(x,t)$ can be rewritten in terms of the averaged velocity $U(x,t)$ and pressure $P(x,t)$ variables [1], [3].

$$\frac{\partial A}{\partial t} + \frac{\partial Q}{\partial x} = 0 \tag{1}$$

$$\frac{\partial Q}{\partial t} + \frac{\partial}{\partial x}\left(\frac{\alpha\, Q^2}{A}\right) + \frac{A}{\rho}\frac{\partial P}{\partial x} = -K_r \frac{Q}{A} \quad . \tag{2}$$

In this system the coefficient α is the so-called momentum flux correction coefficient, and ρ is the fluid density, both are assumed to be constant (in space and time). Parameter K_r is defined using the fluid dynamic viscosity, as the friction parameter, since it reflects the original momentum diffusion term [8], [11]. For the air flow with very low viscosity, the effect of the whole viscous resistance term is close to negligible (confirmed in numerical experiments), thus the value was kept from 3D derivation. Some other model parameters and assumptions with possible higher influence were explored in more details.

4.2 Pressure relation

In order to close the system (1)-(2) a relation for the average (over the cross-section) pressure P in terms of the system variables Q and A has to be provided. Various such pressure-laws have been used in the past. The most common relation applied in studies of blood flow and flow in human upper airways is that used by Formaggia [8] and other authors [7],[10], [13],[9]. This algebraic relation linking pressure P and area A may be written in the general form:

$$P(x,t) - p_{ext} = \psi(A(t,x); A_0(x), \beta(x)), \quad \frac{\partial \psi}{\partial A} > 0, \quad \psi(A_0; A_0; \beta) = 0 \ , \tag{3}$$

where p_{ext} is the external pressure from surrounding tissue. External pressure is set to be zero in the present simulations, but a more realistic value should be prescribed for future experiments.

In the pressure law (3) it is assumed that the pressure depends not only on the wall displacement through the change of section area A, but also on the reference area at rest A_0 (as a deviation of A from the equilibrium state characterized by A_0). The proportionality coefficient β is related to the mechanical properties of the wall. Assuming for simplicity that the pressure is a linear function of the vessel radius we can obtain the following relation [8], [14], [13],[9]

$$\psi(A; A_0; \beta) = \beta \, \frac{\sqrt{A} - \sqrt{A_0}}{A_0}, \quad \text{with} \quad \beta = \frac{\sqrt{\pi} h_0 E}{1 - \kappa_E^2}, \tag{4}$$

where E is the vessel wall Young modulus, κ_E is the corresponding Poisson ratio and h_0 is the wall thickness. As biological tissues are almost incompressible, the Poisson ratio is assumed to be $\kappa_E = 0.49$ for the airways wall. Different other possible laws are discussed in [9].

The relation (4) was originally derived from the full 3D FSI model and it is usually used for the coupling of 3D with 1D FSI models. However, for now, the flow model considered in this work is based on 2D flow in a rigid (planar) channel flow coupled with 1D FSI model. Thus it seems to be reasonable to change and adjust the algebraic relation (4) linking pressure and area to the specific geometry of the 2D model. For example instead of using $\sqrt{A}$ to characterize the cross-sectional radius of a 3D tube, the distance between the walls of a planar channel is denoted directly by A (as it numerically corresponds to the area A).

$$P(A) = p_{ext} + \beta \, \frac{\sqrt{A} - \sqrt{A_0}}{A_0} \quad \xrightarrow[2D]{\text{change for}} \quad P(A) = p_{ext} + \beta \, \frac{A - A_0}{A_0}. \tag{5}$$

This change was tested on several cases and gives better results in the simulations of coupling the 2D and the 1D models. The proportionality (wall elasticity) coefficient β should however be adjusted as well, because the original values were derived from a 3D model (rather than from a 2D model).

5 2D-1D COUPLING STRATEGY

In order to couple the previously described 2D flow and 1D FSI models a specific strategy is needed to bridge the different nature of both models and their implementation. From the naive straightforward perspective it seems to be logical to require that the cross-sectional area A and the global flow rate Q at the common boundary of the 2D model matches at all instants the corresponding values of the attached 1D simplified model. This behavior, although certainly desirable, can not be enforced for the coupled model. The main reason behind this problem comes from the mathematical properties of the 1D FSI model that can be proved to be a hyperbolic system of PDEs, which means (among other issues) that there can be only one boundary condition prescribed at each end of the 1D domain. Thus it is not allowed (not possible) to prescribe both variables A (or P) and Q (or U) at the common 2D-1D coupling interface.

This inability to prescribe both A and Q at the interface, naturally provides two elementary coupling options, resulting in two distinct coupling strategies. In each of them, just one of the quantities is imposed to the 1D model at the coupling interface, while the remaining quantity can only be prescribed at the second, uncoupled end of the 1D domain. The two basic coupling strategies can be summarized as follows:

2D model set up:	**Coupling strategies**
• prescribed $P_0(t), P_2(t)$	• $Q_1(1,t)^{1D} = Q_1(end,t)^{2D}$ $\quad P_1(end,t)^{2D} = P_1(1,t)^{1D}$
• prescribed $U_0(t), P_2(t)$	• $P_1(1,t)^{1D} = P_1(end,t)^{2D}$ $\quad Q_1(end,t)^{2D} = Q_1(1,t)^{1D}$

The 2D flow model can be driven by a prescribed pressure drop, i.e. by prescribing the pressure $P_0(t)$ and $P_1(t)$ at the two inflow/outflow boundaries of the 2D channel. This set-up

is preferred, because it doesn't requires any a-priori knowledge of the shape of the velocity profile and thus can be used without any change for turbulent and non-Newtonian fluids flows, as well as for the oscillatory (Womersley-like) flows, where the velocity profiles might be quite far from the simple parabolic shape. As an alternative, the velocity profile can be prescribed at one boundary and pressure at the other one. This set-up is less convenient (because of the unknown and varying shape of the velocity profile), but on the other hand it can be used to simply enforce the desired flow rate $Q(t)$ for the whole model.

Assuming now the 2D model is fully set, it provides a complete flow field $u(x, z, t)$ and $p(x, z, t)$. To couple this model and fields to the 1D FSI model we can follow one the two above outlined coupling strategies. In the first one, for example, the already calculated flow rate from the 2D model is imposed as a boundary condition for the attached 1D model at the common interface, $Q_1(1, t)^{1D} = Q_1(end, t)^{2D}$. Simultaneously, the average pressure calculated by the 1D model is imposed as the boundary condition to the corresponding interface of the 2D domain, $P_1(end, t)^{2D} = P_1(1, t)^{1D}$.

The second coupling strategy works the other way around, but it still keeps the same philosophy of exchanging the values between 2D and 1D models. Both coupling strategies are schematically summarized in Fig. 2. In general, the explicit coupling consists of passing, at

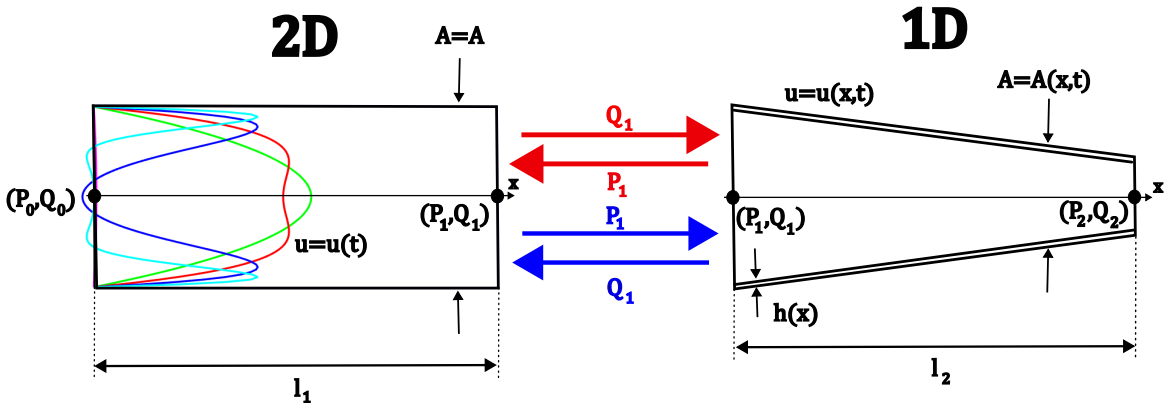

Figure 2: Coupling strategies of 2D with 1D models.

each time step, the flow rate or pressure computed by the 2D model to the 1D solver, which in turn computes and returns the mean pressure P or the flow rate Q, to be fed into the 2D model as a boundary condition. This data exchange procedure repeats at each time step. For simplicity, this procedure is kept explicit in the present simulations, without any internal sub-iterations to enhance the time accuracy and stability.

It is important to remind that as a consequence of the impossibility to prescribe both Q and P at the common coupling interface, inevitably a discontinuity (jump) may occur in one of the quantities. For example, in the first coupling strategy, only the flow rate Q is passed from the 2D to the 1D model, thus the flow rate will remain continuous across the interface. However the pressure P (and consequently A) will be discontinuous on the coupling interface (see [11] for possible fix). Thus the first coupling strategy can also be referred to as *Flow-rate-continuous coupling*[1] , which is the method used to obtain the results presented hereafter.

[1]In contrast to pressure-continuous coupling for the second strategy.

6 NUMERICAL EXPERIMENTS

A series of numerical tests based on the above described coupled model was performed in order to evaluate its sensibility to selected parameters. In the what follows the influence of parameters α and β is discussed in detail.

6.1 Influence of momentum flux correction coefficient α

The momentum flux correction coefficient α is sometimes called Coriolis coefficient. It is defined as the ratio of momentum flux based on actual velocity $u(z)$ to the momentum flux obtained using averaged (constant) velocity profile $\bar{u}$ across a given section. This coefficient, for unidirectional flows of fluids with uniform density can be defined as

$$\alpha = \frac{\int_A \rho u^2 \, dA}{\rho A \bar{u}^2} = \frac{1}{A} \int_A \left(\frac{u}{\bar{u}}\right)^2 dA. \tag{6}$$

Usually the derivation of the coefficient α starts from considering a Poisseuille type of flow, leading to a parabolic velocity profile (in the 3D axisymmetric case). Such parabolic profile can be generalized by allowing higher than quadratic power laws, for more flat velocity profiles found in turbulent or non-Newtonian fluids flows:

$$u(r) = U_{max} \left(1 - \left(\frac{r}{R}\right)^{2\gamma}\right) \text{ , where } \qquad \gamma \geq 1 \text{ ,} \tag{7}$$

where U_{max} is the maximal velocity of the parabolic profile, attained at the center axis where the radial distance $r = 0$. This velocity profile naturally satisfies the no slip condition when the distance r reaches the diameter of the tube, i.e. at $r = R$. It was shown (for example in [1]) that for this type of 3D velocity profile, the average velocity $\bar{u}$

$$\bar{u} = \frac{1}{A} \int_A u(r) \, dA = \frac{1}{\pi R^2} \int_0^R u(r) \, dr = \frac{\gamma}{\gamma + 1} U_{max} \tag{8}$$

and consequently

$$\alpha = \frac{\int_A \rho u^2 \, dA}{\rho A \bar{u}^2} = \frac{1}{A} \int_A \left(\frac{u}{\bar{u}}\right)^2 dA = \frac{2\gamma + 2}{2\gamma + 1} \tag{9}$$

leading in the case of parabolic profile with $\gamma = 1$ to the well known $\bar{u} = \frac{1}{2} U_{max}$ and $\alpha = \frac{4}{3}$.

The 2D model solved in this paper requires similar, but slightly modified procedure, to derive the coefficient α as a function of the velocity profile shape parameter γ. In the 2D planar channel consisting of two infinite parallel plates placed at a distance H, the parabolic profile (emanating from the Poiseuille type flow) can be generalized to:

$$u(z) = U_{max} \left(1 - \left(\frac{z}{H/2}\right)^{2\gamma}\right) \text{ , where } \qquad \gamma \geq 1. \tag{10}$$

For this generalized 2D velocity profile, the average velocity $\bar{u}$ can be calculated as

$$\begin{aligned} \bar{u} = \frac{\int_A u \, dA}{A} = \frac{\int_{-H/2}^{H/2} U_{max} \left(1 - \left(\frac{z}{H/2}\right)^{2\gamma}\right) dz}{H} = \left| \begin{array}{ll} \tilde{z} = \frac{2}{H} z, & z = 0 \Rightarrow \tilde{z} = 0 \\ d\tilde{z} = \frac{2}{H} dz, & z = \frac{H}{2} \Rightarrow \tilde{z} = 1 \end{array} \right| = \\ = \frac{2 U_{max}}{H} \frac{H}{2} \int_0^1 \left(1 - \tilde{z}^{2\gamma}\right) d\tilde{z} = U_{max} \left[\tilde{z} - \frac{\tilde{z}^{2\gamma+1}}{2\gamma + 1}\right]_0^1 = \frac{2\gamma}{2\gamma + 1} \, U_{max} \end{aligned} \tag{11}$$

and similarly the integral

$$\begin{aligned}\int_A u^2\,dA = \int_A U_{max}^2 \left(1-\left(\frac{2z}{H}\right)^{2\gamma}\right)^2 dA = 2U_{max}^2 \int_0^{H/2} \left(1-\left(\frac{2z}{H}\right)^{2\gamma}\right)^2 dz = \\ = \frac{2HU_{max}^2}{2}\int_0^1 \left(1-\tilde{z}^{2\gamma}\right)^2 d\tilde{z} = HU_{max}^2 \int_0^1 \left(1-2\tilde{z}^{2\gamma}+\tilde{z}^{4\gamma}\right) d\tilde{z} = \\ = HU_{max}^2 \left[\tilde{z} - \frac{2\tilde{z}^{2\gamma+1}}{2\gamma+1} + \frac{\tilde{z}^{4\gamma+1}}{4\gamma+1}\right]_0^1 = HU_{max}^2 \left(1-\frac{2}{2\gamma+1}+\frac{1}{4\gamma+1}\right) = \\ = HU_{max}^2 \frac{(2\gamma-1)(4\gamma+1)+2\gamma+1}{(2\gamma+1)(4\gamma+1)} = HU_{max}^2 \frac{8\gamma^2}{(2\gamma+1)(4\gamma+1)}\end{aligned} \tag{12}$$

leading to the final expression for the coefficient α depending on the parameter γ

$$\alpha = \frac{\int_A u^2 dA}{A\,\bar{u}} = \frac{\int_A u^2\,dA}{\int_A \bar{u}^2\,dA} = \frac{HU_{max}^2 \dfrac{8\gamma^2}{(2\gamma+1)(4\gamma+1)}}{HU_{max}^2 \dfrac{4\gamma^2}{(2\gamma+1)^2}} = \frac{4\gamma+2}{4\gamma+1} \tag{13}$$

Again, in the generic case of the parabolic profile with $\gamma = 1$ it leads to $\bar{u} = \frac{2}{3}U_{max}$ and $\alpha = \frac{6}{5}$, which are values just slightly different from those of the 3D case.

For both the classical parabolic (second order) profile in the 3D case ($\alpha = 4/3$) and in the 2D case ($\alpha = 6/5$) the values of the Coriolis parameter are already close to $\alpha = 1$, which is the asymptotic value for flat (constant) velocity profile. Evidently for more flat (than the parabolic) profile, e.g. for shear thinning fluids or for turbulent flows, the physically correct values of the parameter α should be chosen very close to unity. This argument, together with a significant simplification in the derivation and analysis of the 1D model often leads to the a-priori assumption of $\alpha = 1$.

It should be kept in mind that the above described considerations and derivation of the coefficient α were based on steady flow and constant-in-time velocity profile. In the time-periodic case considered in the simulations presented in this paper, such assumption was evidently violated. This is why a series of numerical tests was performed to assess the effects and importance of different choices of the parameter α in the simplified 1D on the solution in the fully resolved coupled 2D model. Results of the velocity gradient, pressure gradient and velocity profiles from the 2D model for different values of the alpha parameter are shown in Fig. 3. These results are compared with the analytical solution and with the solution for a 2D rigid pipe.

When looking into the 1D model results, see Fig. 4, just some transitional effects at the beginning of the simulations are observed, decaying in time and eventually leading to a solution that virtually doesn't differ from the one obtained for $\alpha = 1$.

The results shown in Figs. 3 and 4 document only a marginal effects of different settings of the parameter α. This demonstration justifies the simplification to $\alpha = 1$ also for the time-periodic applications, where the velocity profile is quite far from being parabolic. An open question remains, whether a time-dependent setting for $\alpha(t)$ based on the integration of the Womersley solution (instead of the Poiseuille one) could bring some non-negligible improvement into the simulations.

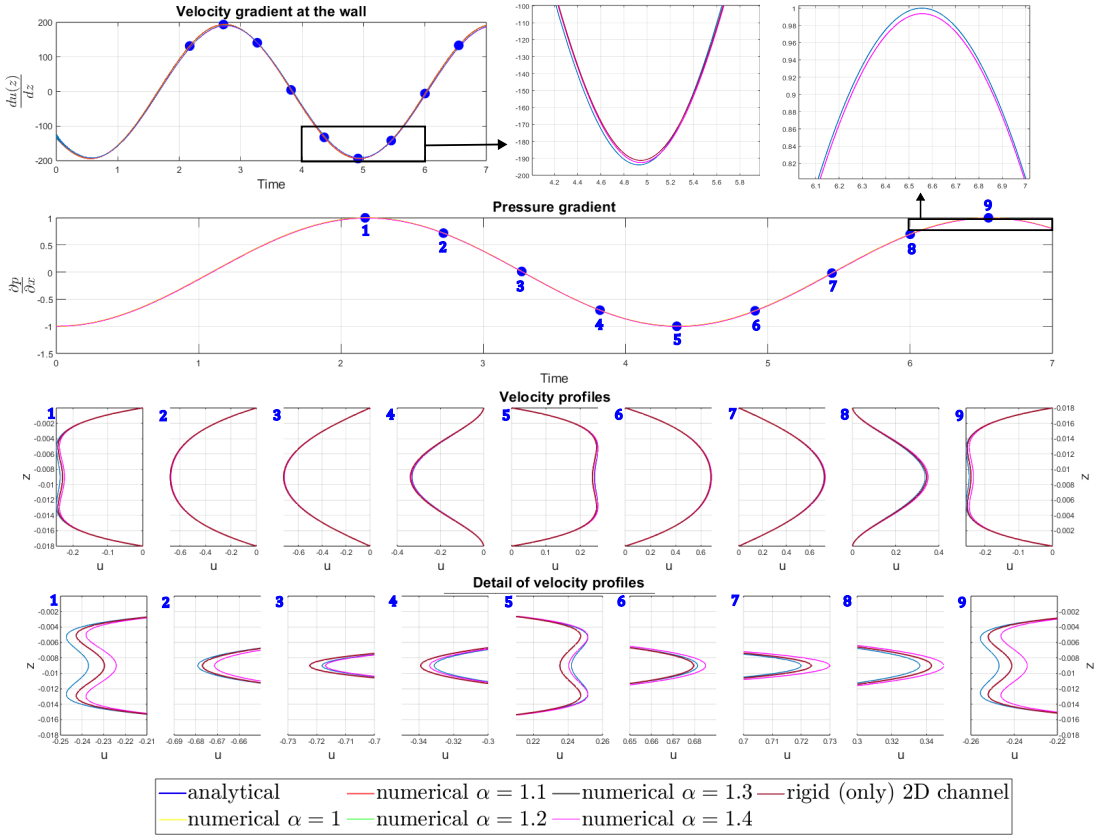

Figure 3: Velocity gradient, pressure gradient and velocity profiles for different values of the parameter α, compared with the analytical (Womersley) solution.

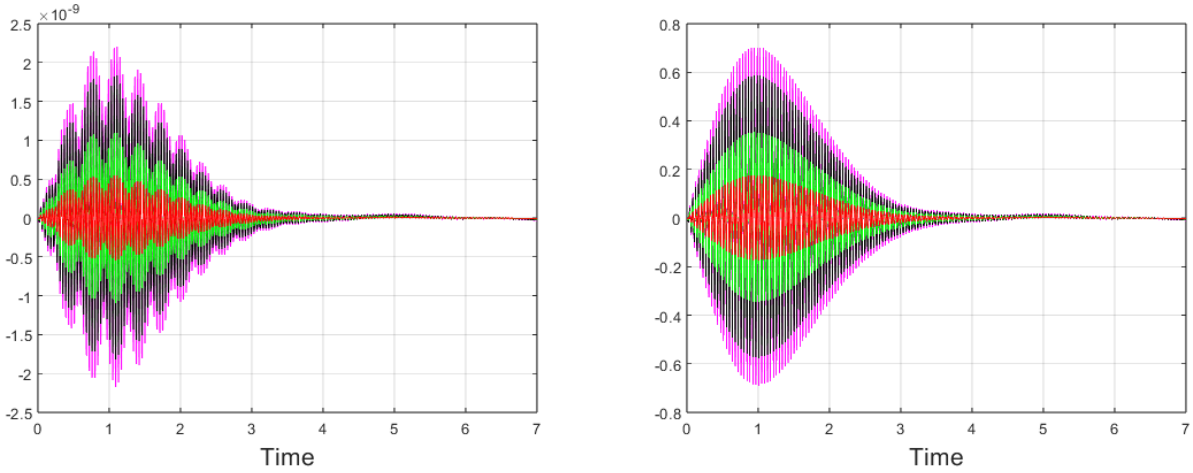

(a) Relative area vs. time at the coupling point.

(b) Pressure drop vs. time in the 1D part.

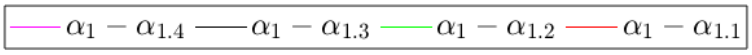

Figure 4: Solution differences in the 1D model for various $\alpha > 1$ compared to $\alpha = 1$.

6.2 Influence of the elasticity coefficient β

The parameter β found previously in the pressure-area laws (3), (4) and (5) represents the elastic behavior of the channel/tube wall. For the 3D axially (rotationally) symmetric tube with thin wall, the parameter can be derived and estimated from the formula mentioned in (4), using the wall thickness h_0, Young's elastic modulus E and Poisson ratio κ_E. This relation however can't simply be transposed into the 2D case, where the geometrical considerations for infinite parallel plates and associated elastic stress differ significantly from those of a tube with circular cross-section. Rather than trying to develop a specific 2D version of the formula for the elasticity parameterβ, only a parameter sensitivity study was performed to show and assess the relative importance of the choice of the parameter β in the 1D FSI model. In order to proceed with such study, a multiplicative (proportionality) factor β_k was introduced to express the value of β in the 2D model as:

$$\beta = \frac{\sqrt{\pi} h_0 E}{1-\kappa_E^2} \qquad \xrightarrow[\text{comparison}]{\text{change for}} \qquad \beta = \beta_k \frac{\sqrt{\pi} h_0 E}{1-\kappa_E^2} \tag{14}$$

In addition, as indicated in (5), also the characteristic area A has to be redefined for the 2D case with parallel plates, rather than using the circular cross-section of the 3D tube case.

$$A_{2D} = H, \qquad \text{instead of} \qquad A_{3D} = \pi R^2 \ . \tag{15}$$

This natural change of $A = H$ in the 2D case, will prevent a significant jump in the pressure gradient between the 2D and 1D models.

The relative importance of the elasticity parameter β in the coupled simulations can be assessed by solving the model for different setting of the proportionality coefficient β_k in (14) .

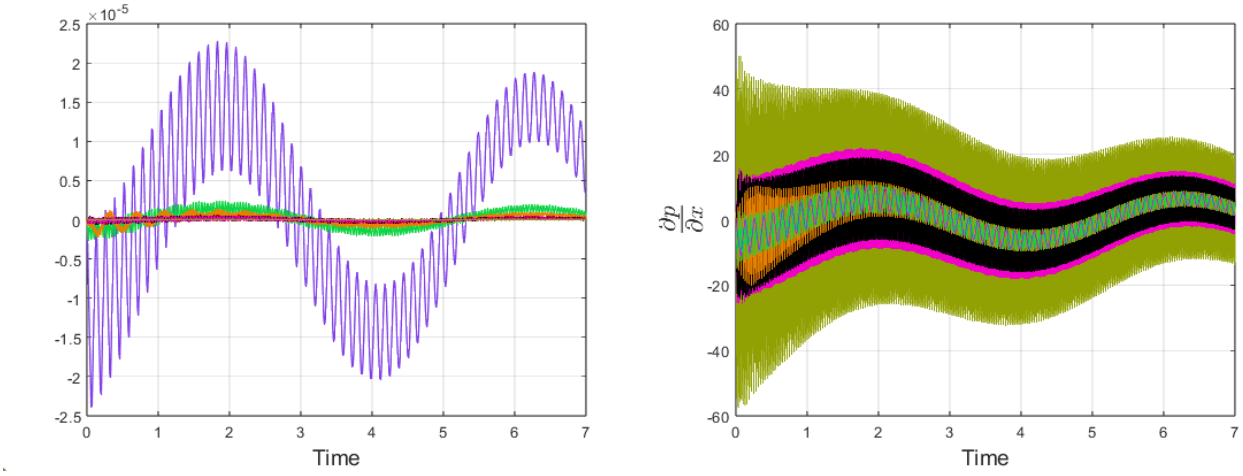

(a) Relative area at the coupling point.

(b) Pressure drop in the 1D part of the model.

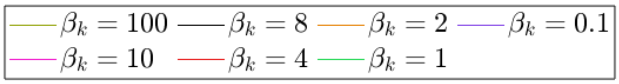

Figure 5: Comparison of results in the 1D model for different values of the factor β_k.

The comparison shown in Fig. 5 for different values of β mainly shows just some transitional effect at the beginning of the simulations, with some low amplitude oscillations superimposed to the solution. Evidently these elastic waves have higher frequency for higher values of β (higher factor β_k).

Although the Fig. 5 shows some differences in the 1D part of the coupled model, the overall effect of different values of β (β_k) on the solution in the 2D domain remains close to negligible, as it can be seen from the comparison of velocity profiles and other quantities shown in Fig. 6.

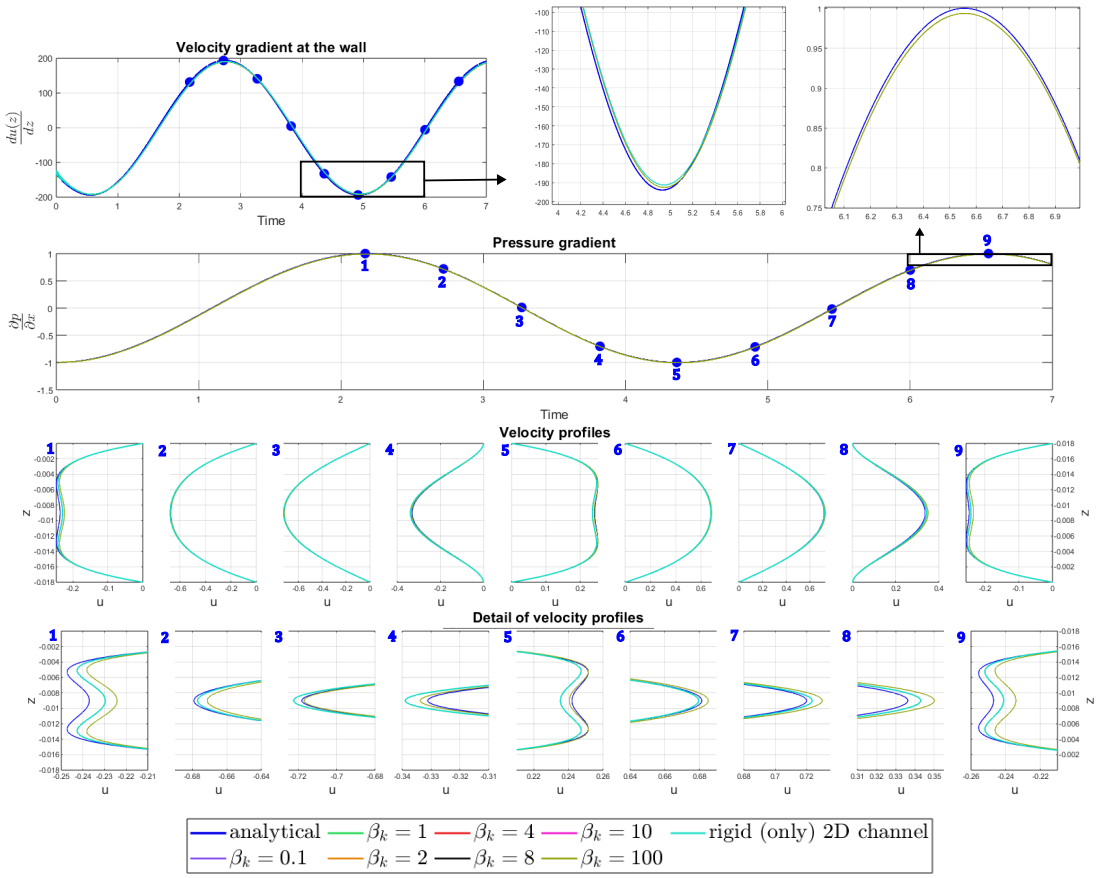

Figure 6: Velocity gradient, pressure gradient and velocity profiles for different values of β, compared with the analytical solution and with a numerical solution for the 2D rigid pipe.

7 CONCLUSIONS

The aim of this paper was to present the 2D-1D explicit flow-FSI coupling procedure with some of the associated implementation problems. The main findings demonstrated in the paper are summarized below:

- The presented explicit coupling procedure for 2D flow and 1D Fluid-Structure-Interaction models proved to be a working concept for this kind of problems. The validation and testing using the time-periodic setup with alternating direction of the flow provided a computational demonstration of the coupled model to be stable and accurate representation of the physical system.

- The parameter sensitivity study dealing with the momentum flux correction parameter α and with the wall elasticity parameter β showed the stability of the numerical methods and the coupling procedure for a wide range of physically relevant values. Although some small differences in the converged solutions were observed, the main differences in the model behavior were just present at the initial stage of the iterative process and fade away in the course of simulations. It means that some attention should be paid to the values of these parameters mainly from the point of view of the simulation start-up and long term stability. Otherwise it is possible to stick with the common values used by other authors. This however might just be the case of the air flow at the considered velocity and pressure conditions, taking into account the relatively low density and viscosity of the air. In other conditions the conclusions may differ substantially from those presented here.

- For the future work a more careful and detailed study of the coupled model stability is scheduled, exploring mainly the hyperbolicity of the 1D FSI model. Such analysis may bring a further insight into an appropriate boundary conditions setup (and thus to the coupling strategy) for the 1D model.

Acknowledgment

The financial support for the present work was partly provided by the European Regional Development Fund - Project "Center for Advanced Applied Science" (No.CZ.02.1.01/0.0/0.0/16 019/0000778), by the *Czech Sciences Foundation* under the *Grant No. GA22-01591S*, and by the *the Praemium Academiae of Š. Nečasová.* A.S. was supported by the *Center for Computational and Stochastic Mathematics - CEMAT (FCT Projects and UIDB/04621/2022 IST-ID)*

REFERENCES

[1] J. Alastruey-Arimon. *Numerical modelling of pulse wave propagation in the cardiovascular system: development, validation and clinical applications.* PhD thesis, Imperial College London, 2006.

[2] A.J. Banko, F. Coletti, C.J. Elkins, and J.K. Eaton. Oscillatory flow in the human airways from the mouth through several bronchial generations. *International Journal of Heat and Fluid Flow*, 61:45–57, 2016.

[3] P.J. Blatz and W.J. Ko. Application of finite elastic theory to the deformation of rubbery materials. *Transactions of the Society of Rheology*, 6(1):223–252, 1962.

[4] T. Bodnár, R. Keslerová, and A. Lancmanová. Numerical investigation of incompressible fluid flow in planar branching channels. In Carapau and Vaidya [5], chapter 5, pages 95–126.

[5] F. Carapau and A. Vaidya, editors. *Recent Advances in Mechanics and Fluid-Structure Interaction with Applications*. Advances in Mathematical Fluid Mechanics. Birkhäuser Cham, 2022.

[6] Clinicalgate. Airflow in the respiratory-system, 2015. https://clinicalgate.com/airflow-in-the-respiratory-system/.

[7] M. Florens, B. Sapoval, and M. Filoche. An anatomical and functional model of the human tracheobronchial tree. *Journal of Applied Physiology*, 110(3):756–763, 2011.

[8] L. Formaggia, A. Quarteroni, and A. Veneziani, editors. *Cardiovascular Mathematics: Modeling and simulation of the circulatory system*. Springer Milano, 2009.

[9] L. Formaggia and A. Veneziani. Reduced and multiscale models for the human cardiovascular system. Technical report, Von Kármán Institute for Fluid Dynamics, Milano, 2003. VKI Lecture Series on Biological Fluid Dynamics.

[10] R.K. Lambert, T.A. Wilson, R.E. Hyatt, and J.R. Rodarte. A computational model for expiratory flow. *Journal of Applied Physiology*, 52(1):44–56, 1982.

[11] A. Lancmanová, T. Bodnár, and A. Sequeira. On the development of a numerical model for the simulation of air flow in the human airways. In *Topical Problems of Fluid Mechanics 2023*, pages 112–118, Prague, 2023. Institute of Thermomechanics CAS.

[12] C. Loudon and A. Tordesillas. The use of the dimensionless womersley number to characterize the unsteady nature of internal flow. *Journal of Theoretical Biology 1998, 191, 63-78.*, 191:63–78, 1998.

[13] A. Quarteroni, A. Veneziani, and C. Vergara. Geometric multiscale modeling of the cardiovascular system, between theory and practice. *Computer Methods in Applied Mechanics and Engineering*, 302:193–252, 2016.

[14] S.J. Sherwin, V. Franke, J. Peiró, and K.H. Parker. One-dimensional modelling of a vascular network in space-time variables. *Journal of Engineering Mathematics*, 47:217–250, 2003.